DEFENSE TECHNICAL INFORMATION CENTER

Information for the Defense Community

DTIC® has determined on 09/14/2004 that this Technical Document has the Distribution Statement checked below. The current distribution for this document can be found in the DTIC® Technical Report Database.

☒ **DISTRIBUTION STATEMENT A.** Approved for public release; distribution is unlimited.

☐ **© COPYRIGHTED**; U.S. Government or Federal Rights License. All other rights and uses except those permitted by copyright law are reserved by the copyright owner.

☐ **DISTRIBUTION STATEMENT B.** Distribution authorized to U.S. Government agencies only (fill in reason) (date of determination). Other requests for this document shall be referred to (insert controlling DoD office)

☐ **DISTRIBUTION STATEMENT C.** Distribution authorized to U.S. Government Agencies and their contractors (fill in reason) (date of determination). Other requests for this document shall be referred to (insert controlling DoD office)

☐ **DISTRIBUTION STATEMENT D.** Distribution authorized to the Department of Defense and U.S. DoD contractors only (fill in reason) (date of determination). Other requests shall be referred to (insert controlling DoD office).

☐ **DISTRIBUTION STATEMENT E.** Distribution authorized to DoD Components only (fill in reason) (date of determination). Other requests shall be referred to (insert controlling DoD office).

☐ **DISTRIBUTION STATEMENT F.** Further dissemination only as directed by (inserting controlling DoD office) (date of determination) or higher DoD authority.

Distribution Statement F is also used when a document does not contain a distribution statement and no distribution statement can be determined.

☐ **DISTRIBUTION STATEMENT X.** Distribution authorized to U.S. Government Agencies and private individuals or enterprises eligible to obtain export-controlled technical data in accordance with DoDD 5230.25; (date of determination). DoD Controlling Office is (insert controlling DoD office).

ORNL/TM-10568

OAK RIDGE
NATIONAL
LABORATORY

MARTIN MARIETTA

DABL69: A Broad-Group Neutron/Photon Cross-Section Library for Defense Nuclear Applications

D. T. Ingersoll
R. W. Roussin
C. Y. Fu
J. E. White

OPERATED BY
MARTIN MARIETTA ENERGY SYSTEMS, INC.
FOR THE UNITED STATES
DEPARTMENT OF ENERGY

ORNL/TM-10568

Engineering Physics and Mathematics

DABL69: A BROAD-GROUP NEUTRON/PHOTON CROSS-SECTION LIBRARY FOR DEFENSE NUCLEAR APPLICATIONS

D. T. Ingersoll
R. W. Roussin
C. Y. Fu
J. E. White

Date Published - June 1989

Work Sponsored by
The Defense Nuclear Agency

Prepared by the
OAK RIDGE NATIONAL LABORATORY
Oak Ridge, Tennessee 37831
operated by
MARTIN MARIETTA ENERGY SYSTEMS, INC.
for the
U.S. DEPARTMENT OF ENERGY
under contract DE-AC05-84OR21400

TABLE OF CONTENTS

LIST OF FIGURES

LIST OF TABLES

ABSTRACT

A new multigroup cross-section library has been generated from ENDF/B-V data for use in defense-related radiation shielding applications. The library is available in a broad-group (46-neutron, 23-photon) energy structure and is designated DABL69. The establishment of specifications for the library, especially the specific group structure and energy weighting functions, was an important part of the generation of the library. The energy group structure contains some special tailoring to the oxygen and nitrogen cross sections and improved energy resolution in the range of 100-1000 keV where the iron cross section is highly structured. The library contains most materials of importance in defense-related shielding problems and includes several reference source spectra and response functions. The library is available in two formats including the commonly used ANISN format and the more versatile AMPX master format.

1. INTRODUCTION

The generation of multigroup cross-section libraries with broad energy group structures is primarily for reasons of economy. It is often not practical to perform two- and three-dimensional radiation transport analyses using pointwise data or finely structured multigroup data. Even for one-dimensional analyses, it is often more efficient to use few-group data to perform the initial scoping analysis and then to advance to finer group data as accuracy requirements are tightened. The establishment of reference broad-group libraries is desirable in order to avoid duplication of effort, both in terms of the library generation and verification, and to assure a common data base for comparisons among program participants.

Uncertainties are inevitably introduced into the broad-group cross sections due to approximations in the grouping procedure. The dominant uncertainty is generally with regard to the energy weighting function used to average the pointwise or fine-group data within a single broad group. Intelligent choice of the weighting functions can reduce such uncertainties. Also, judicious selection of the energy group structure can help to reduce the sensitivity of the computed responses to the weighting function, at least for a selected set of problems. These uncertainties and sensitivities are discussed in later sections with respect to the newly generated broad-group library.

For the last ten years, the radiation transport community for the Defense Nuclear Agency (DNA) has extensively used a reference broad-group library, which is designated DLC-31 by the Radiation Shielding Information Center which maintains and distributes the library.[1] However, it has been recognized for some time that the library is in need of modernization. The current program to reassess doses received by survivors at Hiroshima and Nagasaki, and the recent studies of radiation protection characteristics of armored vehicles have placed particular scrutiny on this library. In addition to the need to incorporate the latest evaluations of the cross-section data, it has been shown that changes to the DLC-31 37-neutron and 21-gamma-ray energy group structure can significantly improve the accuracy of deep-penetration radiation transport calculations, especially when an inadequate number of energy weighting functions are used to generate the broad-group cross sections.

This report describes the procedures used and the specifications for a newly generated cross-section library to be used by the general DNA radiation transport community. The library is designated DABL69, an acronym for Defense Applications Broad-group Library and the total number of energy groups (46 neutron groups and 23 gamma-ray groups). As with the generation of any broad-group library, several compromises had to be made involving: (a) the trade-off between number of energy groups and the amount of computer resources required to use the library, (b) the trade-off between the number of problem-specific energy weighting functions and the bulk size of the library, and (c) the trade-off between flexible data formats

and ease of use in the radiation transport calculations. The rationale used to resolve these trade-offs is given in the next section along with the resulting specifications.

In developing the specifications, an attempt was made to incorporate the experience of several individuals and research groups actively participating in DNA-sponsored programs. In particular, two correspondences[2,3] originating from Science Applications International Corporation (SAIC) provided good summaries of several problems identified with DLC-31, and proposed well-supported fixes. In addition, calculations were performed at ORNL to further study cross-section problems relating to air-over-ground analyses, and to investigate penetration problems other than those addressed in Ref. 2 and 3. The results of these calculations were used to derive the final library specifications, which are presented in Section 2. The final contents of the DABL69 library are listed in Section 3. Several reference source spectra and response functions are included in the library and these are also described in Section 3. Finally, Section 4 gives the results of some calculations similar to the ones used to derive the library specifications. These calculations were performed to test the new library and to demonstrate the importance of the energy group structure and the energy weighting functions.

2. LIBRARY SPECIFICATIONS

2.1. Evaluated Data and Materials

The DLC-31 library is based largely on nuclear data contained in the Evaluated Nuclear Data Files, Version IV (ENDF/B-IV). Since the generation of DLC-31, several improvements have been made to the evaluated data which led to the creation of ENDF/B-V. The new DABL69 library utilizes this data base, except for a few cases noted below where data files even more current than ENDF/B-V were available.

Many of the materials included in ENDF/B-V have previously been processed into a general purpose multigroup library denoted VITAMIN-E.[4] This library achieves generality through: (a) its relatively fine 174-neutron, 38-gamma-ray energy group structure, which largely eliminates the concern for application-dependent energy weighting, and (b) its flexible AMPX[5] data format, which permits problem-dependent processing of the data. The VITAMIN-E library, rather than the ENDF/B-V data files, was used to generate the DABL69 library in order to save considerable effort associated with processing pointwise data into multigroup form. An additional level of reliability is also gained since many of the VITAMIN-E materials have already been used and tested in other applications. The only potential concern for using this approach is that the energy weighting function used to generate the VITAMIN-E multigroup data may not be sufficiently representative for some applications if a high level of accuracy is required. This is not expected to be a concern for most practical problems.

All of the materials currently included in VITAMIN-E are included in DABL69. Although VITAMIN-E contains multiple data sets for some isotopes (due to subsequent updates to the ENDF/B-V files), only the most recent data are included in the DABL69 library. One material requires a special note: The VITAMIN-E library contains a recent reevaluation for iron (sponsored by DNA) which is not an official ENDF/B-V evaluation. This data set is based on the final ENDF/B-V iron data set (Mod 3), but contains significant improvements over the Mod 3 evaluation.[6] This new iron data set has been shown to provide substantially better agreement with integral experiment data and was selected as the best evaluation of iron for inclusion in DABL69.

The full list of materials contained in the DABL69 library is given in Table 1. The list includes all materials which are contained in DLC-31 plus several additional materials. Table 1 also indicates the completeness of the data for each isotope regarding the neutron, photon production, and photon interaction data. It was decided to include photon interaction data in all coupled data sets, even for the few materials for which photon production data do not exist. This could lead to some confusion as to the completeness of the final data and potentially cause erroneous interpretation of results;

TABLE 1. Materials and Data Included In DABL69 Library
(Numbers indicate VITAMIN-E identifiers)

Isotope	Neutron Interaction	Photon Production	Photon Interaction	Included in DLC-31
H-1	930101	130101	1	*
H-2	930202	130202	1	
H-3	116901	--	1	*
He-4	127000	--	2	
Li-6	130301	130301	3	*
Li-7	139701	139701	3	*
Be-9	104	104	4	*
B-10	130501	130501	5	*
B-11	8811	8811	5	*
C-12	130601	130601	6	*
N-14	127501	127501	7	*
O-16	127601	127601	8	*
F-19	130902	130902	9	*
Na-23	131101	131103	11	*
Mg	131201	131201	12	*
Al-27	131301	131301	13	*
Si	131401	131403	14	*
P-31	131501	131501	15	*
S	134701	134701	16	*
Cl	114901	114901	17	*
Ar	8824	8824	18	*
K	115001	115001	19	*
Ca	132003	132003	20	*
Ti	132201	132201	22	*
V	132301	132301	23	*
Cr	132401	132402	24	*
Mn-55	132502	132502	25	*
Fe	932604	932604	26	*
Co-59	132703	132703	27	*
Ni	132802	132801	28	*
Cu	132901	132901	29	*
Ga	135801	135801	31	
Y-89	920201	--	39	
Zr	8841	8841	40	*
Nb-93	118901	118901	41	
Mo	132101	132101	42	*
Cd	8847	8847	48	*
Sn	8850	8850	50	
I-127	960601	--	53	

TABLE 1. Cont'd

Isotope	Neutron Interaction	Photon Production	Photon Interaction	Included in DLC-31
Cs-133	135501	--	55	
Cs-137	966901	--	55	
Ba-138	135301	135301	56	*
Gd	8853	8853	64	*
Hf-174	137401	--	72	
Hf-176	137601	--	72	
Hf-177	137701	--	72	
Hf-178	137801	--	72	
Hf-179	138301	--	72	
Hf-180	138401	--	72	
Ta-181	128502	128502	73	*
W-182	182	182	74	*
W-183	183	183	74	*
W-184	184	184	74	*
W-186	186	186	74	*
Re-185	108301	--	75	
Re-187	108401	--	75	
Pt	8860	8860	78	
Au-197	8861	8861	79	*
Pb	138202	138202	82	*
Bi-209	137501	137501	83	
Th-232	139001	139001	90	
Pa-233	139101	--	91	
U-233	139301	--	92	
U-234	9394	--	92	
U-235	139501	139501	92	*
U-236	139601	--	92	
U-238	139801	139801	92	*
Np-237	133701	--	93	*
Pu-238	133801	--	94	
Pu-239	139901	139901	94	*
Pu-240	138001	138001	94	*
Pu-241	138101	138101	94	
Pu-242	134201	134201	94	
Am-241	136101	136101	95	
Am-242	854201	--	95	
Am-242m	136901	136901	95	
Am-243	136301	136301	95	
Cm-242	864201	864201	96	
Cm-243	134301	134301	96	
Cm-244	134401	134401	96	

however, the absence of the photon production data is clearly noted in this report and also in the library files.

2.2. Group Structure

There are several constraints and desirables which must be balanced when deciding on an energy group structure. In this case, it would have been convenient to retain the 37-neutron, 21-gamma-ray group structure of DLC-31; however, substantial evidence had been accumulated which suggested the need for additional group boundaries, especially in the range of 0.2 to 1.8 MeV. Clearly, the DABL69 group structure must be a subset of the parent VITAMIN-E structure, and it was viewed as desirable to make the new structure a superset of the DLC-31 structure. This latter feature facilitates comparisons of the new data with previously used data.

A 45-neutron, 22-gamma-ray group structure proposed in Ref. 3 appeared to represent a reasonable solution to the difficulties encountered with the DLC-31 structure for air-over-ground applications. The present study began with this 45n/22γ group structure and further investigated its adequacy for some typical shielded vehicle applications. As a result, one of the 45 neutron group boundaries was eliminated, 2 neutron boundaries were added, and one gamma-ray boundary was added yielding the final DABL69 group structure containing 46-neutron and 23-gamma-ray groups. The 46n/23γ structure is given in Tables 2 and 3 compared to the VITAMIN-E and DLC-31 structures. These structures are also shown graphically in Figs. 1 and 2.

Specific differences between the 46n/23γ and earlier 37n/21γ structures include: (a) the addition of neutron boundaries at 1.4227, 0.9616, 0.8209, 0.7427, 0.6393, 0.3688, and 0.2472 MeV to give better energy resolution in the region where the largest fraction of the total kerma frequently occurs, (b) the addition of a boundary at 34.307 keV to better delineate the resonance and window structure of the iron total cross section, (c) the addition of a boundary at 275.36 eV to remove a relatively large lethargy spacing, (d) the extension of the gamma-ray boundaries to 20.0 MeV to permit a proper energy balance when high-energy neutron capture exists, and (e) the addition of a gamma-ray group boundary at 12.0 MeV to better define the nitrogen secondary gamma-ray spectrum.

Unfortunately, one of the group boundaries in the DLC-31 structure does not exactly correspond to any of the boundaries in the VITAMIN-E structure. In particular, the upper group boundary for DLC-31 group 6 is 12.84 MeV while the nearest boundaries in VITAMIN-E are 13.499 and 12.523 MeV. It was decided to use the 12.523-MeV boundary as the substitute for the 12.84-MeV boundary because it gives the smaller shift in energy, and because 12.523 MeV is used as a break-point in the VITAMIN-E weighting function.

TABLE 2. Neutron Group Structure For DLC-31 and New Library Relative To VITAMIN-E Energy Boundaries

VITAMIN-E Group	Upper Energy Boundary (ev)	DLC-31 Group	DABL69 Group
1	1.9640(+07)	1	1
2	1.7332(+07)		
3	1.6905(+07)	2	2
4	1.6487(+07)		
5	1.5683(+07)		
6	1.4918(+07)	3	3
7	1.4550(+07)		
8	1.4191(+07)	4	4
9	1.3840(+07)	5	5
10	1.3499(+07)		
11	1.2523(+07)	6	6
12	1.2214(+07)	7	7
13	1.1618(+07)		
14	1.1052(+07)	8	8
15	1.0513(+07)		
16	1.0000(+07)	9	9
17	9.5123(+06)		
18	9.0484(+06)	10	10
19	8.6071(+06)		
20	8.1873(+06)	11	11
21	7.7880(+06)		
22	7.4082(+06)	12	12
23	7.0469(+06)		
24	6.7032(+06)		
25	6.5924(+06)		
26	6.3763(+06)	13	13
27	6.0653(+06)		
28	5.7695(+06)		
29	5.4881(+06)		
30	5.2205(+06)		
31	4.9659(+06)	14	14
32	4.7237(+06)	15	15
33	4.4933(+06)		
34	4.0657(+06)	16	16
35	3.6788(+06)		
36	3.3287(+06)		
37	3.1664(+06)		

TABLE 2. Cont'd

VITAMIN-E Group	Upper Energy Boundary (ev)	DLC-31 Group	DABL69 Group
38	3.0119(+06)	17	17
39	2.8650(+06)		
40	2.7253(+06)		
41	2.5924(+06)		
42	2.4660(+06)		
43	2.3852(+06)	18	18
44	2.3653(+06)		
45	2.3457(+06)		
46	2.3069(+06)	19	19
47	2.2313(+06)		
48	2.1225(+06)		
49	2.0190(+06)		
50	1.9205(+06)		
51	1.8268(+06)	20	20
52	1.7377(+06)		
53	1.6530(+06)		
54	1.5724(+06)		
55	1.4957(+06)		
56	1.4227(+06)		21
57	1.3534(+06)		
58	1.2874(+06)		
59	1.2246(+06)		
60	1.1648(+06)		
61	1.1080(+06)	21	22
62	1.0026(+06)		
63	9.6164(+05)		23
64	9.0718(+05)		
65	8.6294(+05)		
66	8.2085(+05)		24
67	7.8082(+05)		
68	7.4274(+05)		25
69	7.0651(+05)		
70	6.7206(+05)		
71	6.3928(+05)		26
72	6.0810(+05)		
73	5.7844(+05)		
74	5.5023(+05)	22	27
75	5.2340(+05)		
76	4.9787(+05)		
77	4.5049(+05)		
78	4.0762(+05)		

TABLE 2. Cont'd

VITAMIN-E Group	Upper Energy Boundary (ev)	DLC-31 Group	DABL69 Group
79	3.8774(+05)		
80	3.6883(+05)		28
81	3.3373(+05)		
82	3.0197(+05)		
83	2.9849(+05)		
84	2.9721(+05)		
85	2.9452(+05)		
86	2.8725(+05)		
87	2.7324(+05)		
88	2.4724(+05)		29
89	2.3518(+05)		
90	2.2371(+05)		
91	2.1280(+05)		
92	2.0242(+05)		
93	1.9255(+05)		
94	1.8316(+05)		
95	1.7422(+05)		
96	1.6573(+05)		
97	1.5764(+05)	23	30
98	1.4996(+05)		
99	1.4264(+05)		
100	1.3569(+05)		
101	1.2907(+05)		
102	1.2277(+05)		
103	1.1679(+05)		
104	1.1109(+05)	24	31
105	9.8037(+04)		
106	8.6517(+04)		
107	8.2503(+04)		
108	7.9499(+04)		
109	7.1998(+04)		
110	6.7379(+04)		
111	5.6562(+04)		
112	5.2475(+04)	25	32
113	4.6309(+04)		
114	4.0868(+04)		
115	3.4307(+04)		33
116	3.1828(+04)		
117	2.8501(+04)		
118	2.7000(+04)		
119	2.6058(+04)		

TABLE 2. Cont'd

VITAMIN-E Group	Upper Energy Boundary (ev)	DLC-31 Group	DABL69 Group
120	2.4788(+04)	26	34
121	2.4176(+04)		
122	2.3579(+04)		
123	2.1875(+04)	27	35
124	1.9305(+04)		
125	1.5034(+04)		
126	1.1709(+04)		
127	1.0333(+04)	28	36
128	9.1188(+03)		
129	7.1017(+03)		
130	5.5308(+03)		
131	4.3074(+03)		
132	3.7074(+03)		
133	3.3546(+03)	29	37
134	3.0354(+03)		
135	2.7465(+03)		
136	2.6126(+03)		
137	2.4852(+03)		
138	2.2487(+03)		
139	2.0347(+03)		
140	1.5846(+03)		
141	1.2341(+03)	30	38
142	9.6112(+02)		
143	7.4852(+02)		
144	5.8295(+02)	31	39
145	4.5400(+02)		
146	3.5357(+02)		
147	2.7536(+02)		40
148	2.1445(+02)		
149	1.6702(+02)		
150	1.3007(+02)		
151	1.0130(+02)	32	41
152	7.8893(+01)		
153	6.1442(+01)		
154	4.7851(+01)		
155	3.7267(+01)		
156	2.9023(+01)	33	42
157	2.2603(+01)		
158	1.7603(+01)		
159	1.3710(+01)		

TABLE 2. Cont'd

VITAMIN-E Group	Upper Energy Boundary (ev)	DLC-31 Group	DABL69 Group
160	1.0677(+01)	34	43
161	8.3153(+00)		
162	6.4759(+00)		
163	5.0435(+00)		
164	3.9279(+00)		
165	3.0590(+00)	35	44
166	2.3824(+00)		
167	1.8554(+00)		
168	1.4450(+00)		
169	1.1253(+00)	36	45
170	8.7642(-01)		
171	6.8256(-01)		
172	5.3158(-01)		
173	4.1399(-01)	37	46
174	1.0000(-01)		
	1.0000(-05)[a]		

[a] Lower energy boundary of last group.

TABLE 3. Gamma-Ray Group Structure of DLC-31 and New Library Relative to VITAMIN-E Energy Boundaries

VITAMIN-E Group	Upper Energy Boundary (ev)	DLC-31 Group	DABL69 Group
1	2.0000(+07)		1
2	1.4000(+07)	1	2
3	1.2000(+07)		3
4	1.0000(+07)	2	4
5	8.0000(+06)	3	5
6	7.5000(+06)		
7	7.0000(+06)	4	6
8	6.5000(+06)		
9	6.0000(+06)	5	7
10	5.5000(+06)		
11	5.0000(+06)	6	8
12	4.5000(+06)		
13	4.0000(+06)	7	9
14	3.5000(+06)		
15	3.0000(+06)	8	10
16	2.5000(+06)	9	11
17	2.0000(+06)	10	12
18	1.6600(+06)		
19	1.5000(+06)	11	13
20	1.3300(+06)		
21	1.0000(+06)	12	14
22	8.0000(+05)		
23	7.0000(+05)	13	15
24	6.0000(+05)		
25	5.1200(+05)		
26	5.1000(+05)		
27	4.5000(+05)	14	16
28	4.0000(+05)		
29	3.0000(+05)	15	17
30	2.0000(+05)		
31	1.5000(+05)	16	18
32	1.0000(+05)	17	19
33	7.5000(+04)		
34	7.0000(+04)	18	20
35	6.0000(+04)		
36	4.5000(+04)	19	21
37	3.0000(+04)	20	22
38	2.0000(+04)	21	23
	1.0000(+04)[a]		

[a] Lower energy boundary of last group.

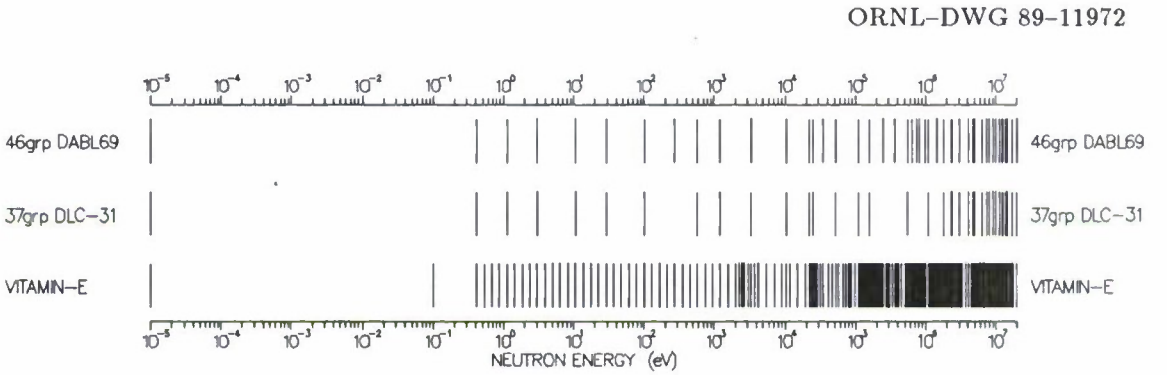

Fig. 1. Graphic representation of neutron energy group boundaries.

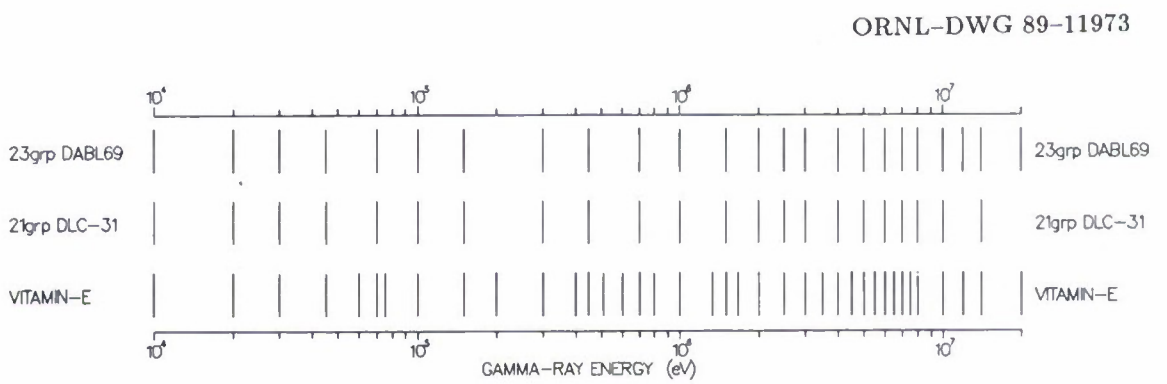

Fig. 2. Graphic representation of gamma-ray energy group boundaries.

As a point of clarification, it has been often noted (including in Ref. 2) that a second mis-match of boundaries also occurs at nominally 10.4 keV. However, other evidence showed that no mis-match occurs. Confusion on this issue results from the fact that during the preparation of VITAMIN-E, the neutron cross sections were prepared with an upper energy boundary of 10.333 keV for group 127, while the photon production cross sections were prepared with an energy of 10.595 keV for this group. This discrepancy of boundaries has no impact for those isotopes which have flat photon multiplicities in the vicinity of this energy, and has only minor impact for those isotopes with changing multiplicities. Nonetheless, this error in the VITAMIN-E library was corrected prior to generation of DABL69. Hence, both the corrected VITAMIN-E library and the DABL69 library contain the proper boundary at 10.333 keV in order to exactly correspond with the DLC-31 group 28 boundary.

2.3. Weighting Functions

It has been clearly shown that the use of only a single energy weighting function to collapse cross sections to a broad-group level can generate significant inaccuracies for deep penetration problems. For these cases, or when stringent requirements for accuracy exist, one must use fine-group cross sections or prepare numerous broad-group sets collapsed using representative flux spectra. However, the vast number of potential variables preclude the use of problem-dependent weighting functions for the generation of a general purpose cross-section library.

The DABL69 library contains cross sections which have been collapsed using a single "standard" weighting function and two problem-dependent weighting functions. For the neutron interaction and photon production data, these functions include:

1. A weighting spectrum which is the multigroup form of the energy weighting function used to create the VITAMIN-E data from ENDF/B-V. It is a smoothly varying function consisting of a 300 K Maxwellian, a 1.4-MeV fission spectrum, and a 14.07-MeV fusion peak spectrum overlaid on a 1/E slowing-down spectrum. The function is detailed in Table 4 and is shown in Fig. 3. All materials in the new library were collapsed using this function.

2. A spectrum representing neutron transport from a fission source through infinite air. Only hydrogen, oxygen, and nitrogen were collapsed using this function. The spectrum was determined by calculating the transport of neutrons from a ^{252}Cf fission source through 3000 m of air. The weighting function was then taken to be the group fluxes at 2000 m. This weighting function is also given in Table 4 and shown in Fig. 3.

TABLE 4. Energy Weighting Functions Used To Collapse VITAMIN-E Neutron Cross Sections

Group	Upper Bound (eV)	Standard Spectrum	Infinite Air	Stainless Steel
1	1.96403(+7)	7.9664(-3)	2.9696(-7)	4.1348(-2)
2	1.73325(+7)	1.5932(-3)	7.8045(-8)	8.0911(-3)
3	1.69046(+7)	1.5933(-3)	9.9458(-8)	7.9950(-3)
4	1.64872(+7)	3.1865(-3)	2.7645(-7)	1.5644(-2)
5	1.56831(+7)	3.1246(-1)	1.6055(-7)	1.4824
6	1.49183(+7)	2.1349	1.9314(-7)	9.9897
7	1.45499(+7)	6.4200	2.6756(-7)	2.9648(+1)
8	1.41907(+7)	8.3253	3.5379(-7)	3.7943(+1)
9	1.38403(+7)	4.7866	4.5340(-7)	2.1549(+1)
10	1.34986(+7)	1.4090	3.6155(-6)	6.2478
11	1.25232(+7)	9.2058(-4)	5.0066(-7)	3.9323(-3)
12	1.22140(+7)	1.8408(-3)	2.1621(-6)	7.6924(-3)
13	1.16183(+7)	1.8407(-3)	3.9234(-6)	7.4555(-3)
14	1.10517(+7)	1.8408(-3)	7.3847(-6)	7.2704(-3)
15	1.05127(+7)	1.8408(-3)	1.0361(-5)	7.1288(-3)
16	1.00000(+7)	2.1201(-3)	2.1057(-5)	8.0527(-3)
17	9.51229(+6)	2.7618(-3)	4.1964(-5)	1.0256(-2)
18	9.04837(+6)	3.5387(-3)	5.7060(-5)	1.2974(-2)
19	8.60708(+6)	4.4634(-3)	8.9259(-5)	1.5816(-2)
20	8.18731(+6)	5.5463(-3)	7.1937(-5)	1.9390(-2)
21	7.78801(+6)	6.7943(-3)	7.4295(-5)	2.3328(-2)
22	7.40818(+6)	8.2113(-3)	8.4002(-5)	2.7722(-2)
23	7.04688(+6)	9.7968(-3)	2.5769(-4)	3.2789(-2)
24	6.70320(+6)	3.6472(-3)	1.1014(-4)	1.2062(-2)
25	6.59238(+6)	7.8988(-3)	3.1672(-4)	2.5947(-2)
26	6.37628(+6)	1.3450(-2)	4.7050(-4)	4.4471(-2)
27	6.06531(+6)	1.5495(-2)	5.1564(-4)	5.0576(-2)
28	5.76950(+6)	1.7663(-2)	4.9073(-4)	5.7398(-2)
29	5.48812(+6)	1.9934(-2)	6.2308(-4)	6.4413(-2)
30	5.22046(+6)	2.2283(-2)	6.9706(-4)	7.1989(-2)
31	4.96585(+6)	2.4684(-2)	2.4246(-3)	7.9141(-2)
32	4.72367(+6)	2.7108(-2)	1.4339(-3)	8.6282(-2)
33	4.49329(+6)	6.1435(-2)	1.4133(-3)	1.9613(-1)
34	4.06570(+6)	7.0689(-2)	1.0697(-3)	2.2913(-1)
35	3.67879(+6)	7.9125(-2)	9.8668(-4)	2.6596(-1)
36	3.32871(+6)	4.2370(-2)	5.2877(-4)	1.4419(-1)
37	3.16637(+6)	4.4015(-2)	6.6502(-4)	1.4670(-1)
38	3.01194(+6)	4.5473(-2)	6.9728(-4)	1.5902(-1)
39	2.86505(+6)	4.6732(-2)	1.0015(-3)	1.6026(-1)
40	2.72532(+6)	4.7789(-2)	1.1122(-3)	1.6598(-1)

TABLE 4. Cont'd

Group	Upper Bound (eV)	Standard Spectrum	Infinite Air	Stainless Steel
41	2.59240(+6)	4.8637(-2)	1.2702(-3)	1.5648(-1)
42	2.46597(+6)	3.2760(-2)	1.1325(-3)	1.1015(-1)
43	2.38521(+6)	8.3024(-3)	3.7242(-4)	3.2512(-2)
44	2.36525(+6)	8.2155(-3)	4.1371(-4)	3.5792(-2)
45	2.34570(+6)	1.6566(-2)	7.9991(-4)	5.7884(-2)
46	2.30686(+6)	3.3147(-2)	1.1060(-3)	1.2975(-1)
47	2.23130(+6)	4.9946(-2)	1.6342(-3)	1.8568(-1)
48	2.12248(+6)	5.0000(-2)	1.8128(-3)	1.7663(-1)
49	2.01897(+6)	5.0000(-2)	1.8186(-3)	1.9044(-1)
50	1.92050(+6)	5.0000(-2)	1.6806(-3)	2.0426(-1)
51	1.82684(+6)	5.0000(-2)	1.5352(-3)	2.0944(-1)
52	1.73774(+6)	5.0000(-2)	1.7677(-3)	2.1220(-1)
53	1.65299(+6)	5.0000(-2)	1.3851(-3)	1.9953(-1)
54	1.57237(+6)	5.0000(-2)	1.8111(-3)	1.8780(-1)
55	1.49569(+6)	5.0000(-2)	1.8115(-3)	1.8582(-1)
56	1.42274(+6)	5.0000(-2)	1.6378(-3)	2.2558(-1)
57	1.35335(+6)	5.0000(-2)	1.5830(-3)	1.9437(-1)
58	1.28735(+6)	5.0000(-2)	2.5759(-3)	1.9107(-1)
59	1.22456(+6)	5.0000(-2)	2.6037(-3)	2.6178(-1)
60	1.16484(+6)	5.0000(-2)	1.8345(-3)	2.4047(-1)
61	1.10803(+6)	1.0000(-1)	3.2135(-3)	4.6566(-1)
62	1.00259(+6)	4.1700(-2)	1.5713(-3)	1.7349(-1)
63	9.61640(+5)	5.8300(-2)	3.1172(-3)	3.3309(-1)
64	9.07180(+5)	5.0000(-2)	2.6843(-3)	2.1028(-1)
65	8.62936(+5)	5.0000(-2)	2.9834(-3)	2.3471(-1)
66	8.20850(+5)	5.0000(-2)	3.2344(-3)	1.7544(-1)
67	7.80817(+5)	5.0000(-2)	3.0488(-3)	1.5814(-1)
68	7.42736(+5)	5.0000(-2)	2.8524(-3)	2.2025(-1)
69	7.06512(+5)	5.0000(-2)	2.7312(-3)	2.4945(-1)
70	6.72055(+5)	5.0000(-2)	2.7043(-3)	2.8346(-1)
71	6.39279(+5)	5.0000(-2)	3.9597(-3)	2.5347(-1)
72	6.08101(+5)	5.0000(-2)	3.9380(-3)	2.7585(-1)
73	5.78443(+5)	5.0000(-2)	3.6753(-3)	1.9943(-1)
74	5.50232(+5)	5.0000(-2)	3.5632(-3)	2.0194(-1)
75	5.23397(+5)	5.0000(-2)	3.4114(-3)	1.7515(-1)
76	4.97871(+5)	1.0000(-1)	5.0688(-3)	3.6686(-1)
77	4.50492(+5)	1.0000(-1)	4.0340(-3)	2.7496(-1)
78	4.07622(+5)	5.0000(-2)	2.2706(-3)	1.4156(-1)
79	3.87742(+5)	5.0000(-2)	2.1762(-3)	2.2613(-1)
80	3.68832(+5)	1.0000(-1)	5.0125(-3)	4.5679(-1)

TABLE 4. Cont'd

Group	Upper Bound (eV)	Standard Spectrum	Infinite Air	Stainless Steel
81	3.33733(+5)	1.0000(-1)	5.2944(-3)	5.2442(-1)
82	3.01974(+5)	1.1600(-2)	6.0649(-4)	7.7160(-2)
83	2.98491(+5)	4.3000(-3)	2.2492(-4)	2.5269(-2)
84	2.97210(+5)	9.1000(-3)	4.7637(-4)	4.7310(-2)
85	2.94518(+5)	2.5000(-2)	1.3134(-3)	1.0017(-1)
86	2.87247(+5)	5.0000(-2)	2.6542(-3)	1.7194(-1)
87	2.73237(+5)	1.0000(-1)	5.3542(-3)	4.3568(-1)
88	2.47235(+5)	5.0000(-2)	2.6850(-3)	1.7737(-1)
89	2.35177(+5)	5.0000(-2)	2.6882(-3)	1.6899(-1)
90	2.23708(+5)	5.0000(-2)	2.6989(-3)	1.8329(-1)
91	2.12797(+5)	5.0000(-2)	2.7089(-3)	1.3312(-1)
92	2.02419(+5)	5.0000(-2)	2.7107(-3)	1.0786(-1)
93	1.92547(+5)	5.0000(-2)	2.7120(-3)	1.3740(-1)
94	1.83156(+5)	5.0000(-2)	2.7147(-3)	2.1654(-1)
95	1.74224(+5)	5.0000(-2)	2.7186(-3)	1.5427(-1)
96	1.65727(+5)	5.0000(-2)	2.7186(-3)	1.4560(-1)
97	1.57644(+5)	5.0000(-2)	2.7184(-3)	1.3066(-1)
98	1.49956(+5)	5.0000(-2)	2.7192(-3)	7.3300(-2)
99	1.42642(+5)	5.0000(-2)	2.7201(-3)	1.5816(-1)
100	1.35686(+5)	5.0000(-2)	2.7159(-3)	2.2159(-1)
101	1.29068(+5)	5.0000(-2)	2.7119(-3)	2.2878(-1)
102	1.22773(+5)	5.0000(-2)	2.7094(-3)	2.1872(-1)
103	1.16786(+5)	5.0000(-2)	2.7070(-3)	1.6227(-1)
104	1.11090(+5)	1.2500(-1)	6.7388(-3)	2.5929(-1)
105	9.80365(+4)	1.2500(-1)	6.6596(-3)	2.7516(-1)
106	8.65169(+4)	4.7500(-2)	2.5094(-3)	7.0338(-2)
107	8.25034(+4)	3.7099(-2)	1.9490(-3)	2.3847(-1)
108	7.94987(+4)	9.9100(-2)	5.1564(-3)	2.5973(-1)
109	7.19981(+4)	6.6300(-2)	3.4169(-3)	2.3096(-1)
110	6.73794(+4)	1.7500(-1)	8.8507(-3)	4.8173(-1)
111	5.65622(+4)	7.5000(-2)	3.7258(-3)	1.5783(-1)
112	5.24752(+4)	1.2500(-1)	6.1235(-3)	2.3854(-1)
113	4.63092(+4)	1.2500(-1)	6.0170(-3)	3.1304(-1)
114	4.08677(+4)	1.7500(-1)	8.2604(-3)	3.0586(-1)
115	3.43067(+4)	7.5000(-2)	3.4931(-3)	9.2400(-2)
116	3.18278(+4)	1.1040(-1)	5.0957(-3)	6.1909(-2)
117	2.85010(+4)	5.4100(-2)	2.4832(-3)	1.4450(-2)
118	2.70001(+4)	3.5500(-2)	1.6240(-3)	4.8128(-2)
119	2.60584(+4)	5.0000(-2)	2.2803(-3)	2.3946(-1)
120	2.47875(+4)	2.5000(-2)	1.1377(-3)	1.4254(-1)

TABLE 4. Cont'd

Group	Upper Bound (eV)	Standard Spectrum	Infinite Air	Stainless Steel
121	2.41755(+4)	2.5000(-2)	1.1353(-3)	1.1283(-1)
122	2.35786(+4)	7.5000(-2)	3.3932(-3)	3.1954(-1)
123	2.18749(+4)	1.2500(-1)	5.6137(-3)	3.9150(-1)
124	1.93045(+4)	2.5000(-1)	1.1064(-2)	4.1736(-1)
125	1.50344(+4)	2.5000(-1)	1.0987(-2)	3.9108(-1)
126	1.17088(+4)	1.2500(-1)	5.4806(-3)	2.3130(-1)
127	1.03330(+4)	1.2500(-1)	5.4747(-3)	1.9617(-1)
128	9.11881(+3)	2.5000(-1)	1.0956(-2)	1.7720(-1)
129	7.10174(+3)	2.5000(-1)	1.0960(-2)	2.2894(-1)
130	5.53084(+3)	2.5000(-1)	1.0959(-2)	2.4134(-1)
131	4.30742(+3)	1.5000(-1)	6.5651(-3)	1.3314(-1)
132	3.70744(+3)	1.0000(-1)	4.3754(-3)	1.1189(-1)
133	3.35463(+3)	1.0000(-1)	4.3759(-3)	1.2119(-1)
134	3.03539(+3)	1.0000(-1)	4.3696(-3)	1.1787(-1)
135	2.74653(+3)	5.0000(-2)	2.1825(-3)	5.1640(-2)
136	2.61258(+3)	5.0000(-2)	2.1814(-3)	4.2819(-2)
137	2.48517(+3)	1.0000(-1)	4.3608(-3)	7.1200(-2)
138	2.24867(+3)	1.0000(-1)	4.3589(-3)	9.7955(-2)
139	2.03468(+3)	2.5000(-1)	1.0861(-2)	3.1628(-1)
140	1.58461(+3)	2.5000(-1)	1.0819(-2)	3.3243(-1)
141	1.23410(+3)	2.5000(-1)	1.0784(-2)	2.8837(-1)
142	9.61116(+2)	2.5000(-1)	1.0781(-2)	3.1491(-1)
143	7.48518(+2)	2.5000(-1)	1.0781(-2)	3.0294(-1)
144	5.82946(+2)	2.5000(-1)	1.0795(-2)	2.9044(-1)
145	4.53999(+2)	2.5000(-1)	1.0792(-2)	2.3418(-1)
146	3.53575(+2)	2.5000(-1)	1.0785(-2)	1.5687(-1)
147	2.75364(+2)	2.5000(-1)	1.0762(-2)	2.7069(-1)
148	2.14454(+2)	2.5000(-1)	1.0755(-2)	2.7785(-1)
149	1.67017(+2)	2.5000(-1)	1.0715(-2)	2.7771(-1)
150	1.30073(+2)	2.5000(-1)	1.0686(-2)	2.7799(-1)
151	1.01301(+2)	2.5000(-1)	1.0701(-2)	2.7812(-1)
152	7.88932(+1)	2.5000(-1)	1.0739(-2)	2.7807(-1)
153	6.14421(+1)	2.5000(-1)	1.0771(-2)	2.7793(-1)
154	4.78512(+1)	2.5000(-1)	1.0797(-2)	2.7772(-1)
155	3.72665(+1)	2.5000(-1)	1.0813(-2)	2.7746(-1)
156	2.90232(+1)	2.5000(-1)	1.0816(-2)	2.7715(-1)
157	2.26033(+1)	2.5000(-1)	1.0805(-2)	2.7679(-1)
158	1.76034(+1)	2.5000(-1)	1.0780(-2)	2.7639(-1)
159	1.37096(+1)	2.5000(-1)	1.0738(-2)	2.7594(-1)
160	1.06770(+1)	2.5000(-1)	1.0677(-2)	2.7544(-1)

TABLE 4. Cont'd

Group	Upper Bound (eV)	Standard Spectrum	Infinite Air	Stainless Steel
161	8.31529	2.5000(-1)	1.0594(-2)	2.7489(-1)
162	6.47595	2.5000(-1)	1.0485(-2)	2.7428(-1)
163	5.04348	2.5000(-1)	1.0349(-2)	2.7359(-1)
164	3.92786	2.5000(-1)	1.0183(-2)	2.7281(-1)
165	3.05902	2.5000(-1)	9.9843(-3)	2.7194(-1)
166	2.38237	2.5000(-1)	9.7497(-3)	2.7096(-1)
167	1.85539	2.5000(-1)	9.4773(-3)	2.6986(-1)
168	1.44498	2.5000(-1)	9.1651(-3)	2.6861(-1)
169	1.12535	2.5000(-1)	8.8122(-3)	2.6723(-1)
170	8.76425(-1)	2.5000(-1)	8.4178(-3)	2.6568(-1)
171	6.82560(-1)	2.5000(-1)	7.9821(-3)	2.6394(-1)
172	5.31578(-1)	2.5000(-1)	7.5066(-3)	2.6200(-1)
173	4.13994(-1)	3.5783(+3)	9.7781(-3)	3.5395(+3)
174	1.00000(-1)	3.1604(+4)	2.1795(-2)	2.7827(+4)
	1.00000(-5)[a]			

[a] Lower energy boundary of last group.

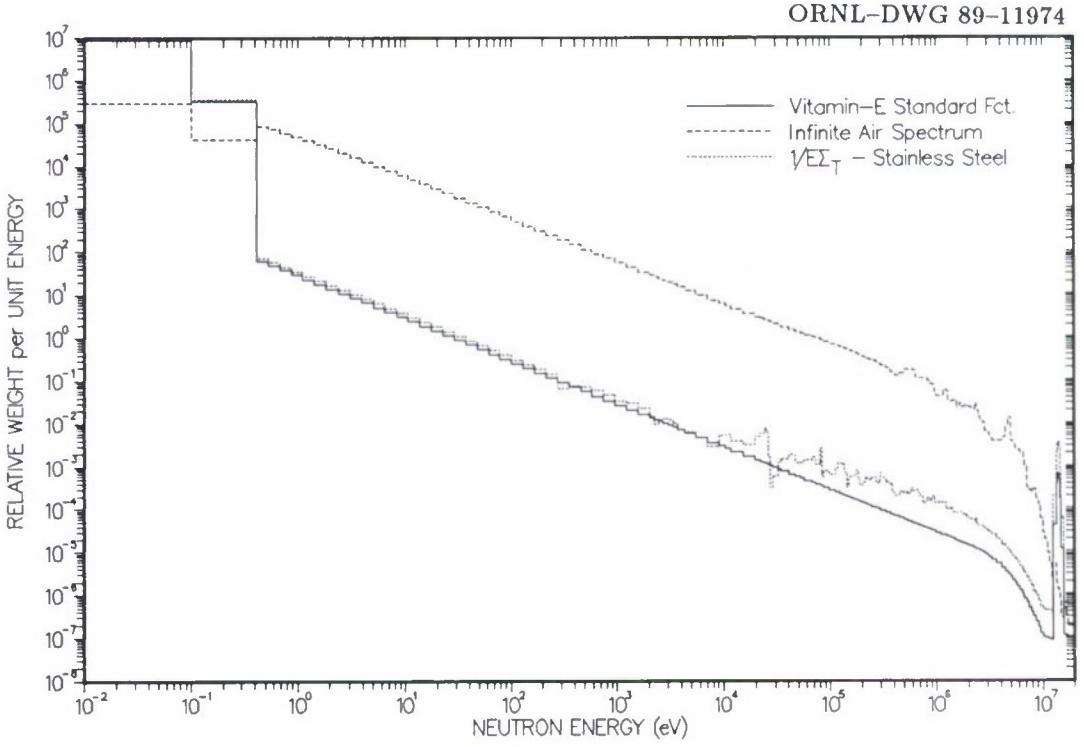

Fig. 3. Energy weighting functions for collapsing neutron cross sections.

3. A spectrum representing the inverse of energy times the total cross section of type-304 stainless steel, $1/[E\Sigma_T(SS)]$ molybdenum. More precisely, this function was derived by groupwise folding the standard weighting function (described in item 1 above) with the inverse of the stainless steel total macroscopic cross section. The resulting function incorporates the spectral features of neutron slowing down and the highly structured shape of the stainless steel cross sections. It is felt that this approach gives a generally acceptable weighting for computing deep-penetration transport through ferrous materials. As above, this weighting function is listed in Table 4 and shown in Fig. 3.

Most typically, a weighting function which is flat in energy is used for gamma-ray interaction cross section libraries developed for shielding applications, and is the type of weighting used in the DLC-31 library. However, calculations performed for this project showed that collapsing the data with an inverse energy weighting (flat in lethargy) yielded better agreement between the fine-group and broad-group responses for representative air-over-ground and shielded geometries. Hence, all of the gamma-ray interaction cross sections in the DABL69 library have been collapsed with a 1/E spectrum.

2.4. Self-Shielding and Order of Scattering

All materials in the DABL69 library were processed as infinitely dilute, i.e. no resonance self-shielding adjustments were made to the cross sections. Additionally, the Cr, Mn, Fe, and Ni data sets which were collapsed using the $1/[E\Sigma_T(SS)]$ weighting function mentioned above were self-shielded for type-304 stainless steel at a density of 7.8 g/cm^3.

A P_5 Legendre expansion of the group-to-group scattering matrix was used for all materials. The VITAMIN-E library contains at least this order of expansion for all gamma-ray interaction data; however, only a portion of the neutron data contain this level of expansion. The materials for which only P_3 data are available include primarily the heavier isotopes and special purpose materials.

2.5. Cross-Section Format

The new library is available in two formats. This includes the standard ANISN[7] format with a table length of 72 (number of groups plus 3). Table positions 1 through 4 are defined as:

1. absorption cross section (σ_a),

2. fission cross section times the number of neutrons produced per fission ($\nu\sigma_f$),

3. total cross section (σ_T), and

4. within-group scattering cross section ($\sigma_{g\to g}$).

These positions are followed by the standard down-scatter transfer matrix.

The cross-section format described above contains some redundency. In particular, the absorption cross-section can be computed from the remaining cross sections and are not directly needed for the solution of the flux equations for some transport codes. As a result, some earlier cross-section libraries have used position 1 for data other than the absorption cross-section. This can lead to confusion, however, such as with the DLC-31 library, which contains absorption data in position 1 for some materials but which contains kerma data in the same position for other materials. Since the creation of DLC-31, modifications were made to the MORSE Monte Carlo code[8] which uses a Klein-Nishina estimator to compute last-flight gamma-ray contributions to a point detector response.[9] To use this method, it is desirable to have the true absorption cross section always present in position 1. For this reason, and to avoid possible confusion, table position 1 in the DABL69 library contains only the absorption cross section.

The DABL69 library is also available in the AMPX master format.[5] This format is more flexible than the ANISN format, but it is not directly usable for most standard radiation transport codes. Its value is in the fact that all the various partial cross sections are retained in separate records and can be retrieved as needed for special purposes. Also, additional temperature-dependent self-shielding parameters exist in the files so that problem-dependent cross sections can be readily prepared. Hence, the AMPX-formatted version of the library is important for addressing special applications.

2.6. Cross-Section Processing

The AMPX Modular Code System[5] was used to prepare DABL69. Several system modules were employed including:

Module	Function
AJAX	To select particular data sets for special processing and recombine them later with the full library
CHOX	Combine neutron, photon production, and photon interaction data
AXMIX	Merge multiple libraries and prepare macroscopic

	cross sections
BONAMI	Perform resonance self-shielding on constituents of steel
MALOCS	Collapse coupled library from 174n/38γ groups to 46n/23γ groups
NITAWL	Convert from AMPX master format to AMPX working format
ALPO	Convert from AMPX working format to ANISN format
VEL	Convert pointwise data to multigroup form (used for preparing some response functions)
RADE	Perform several checks on final library

A flow diagram depicting the full procedure used to generate DABL69 is shown in Fig. 4.

ORNL-DWG 89-11975

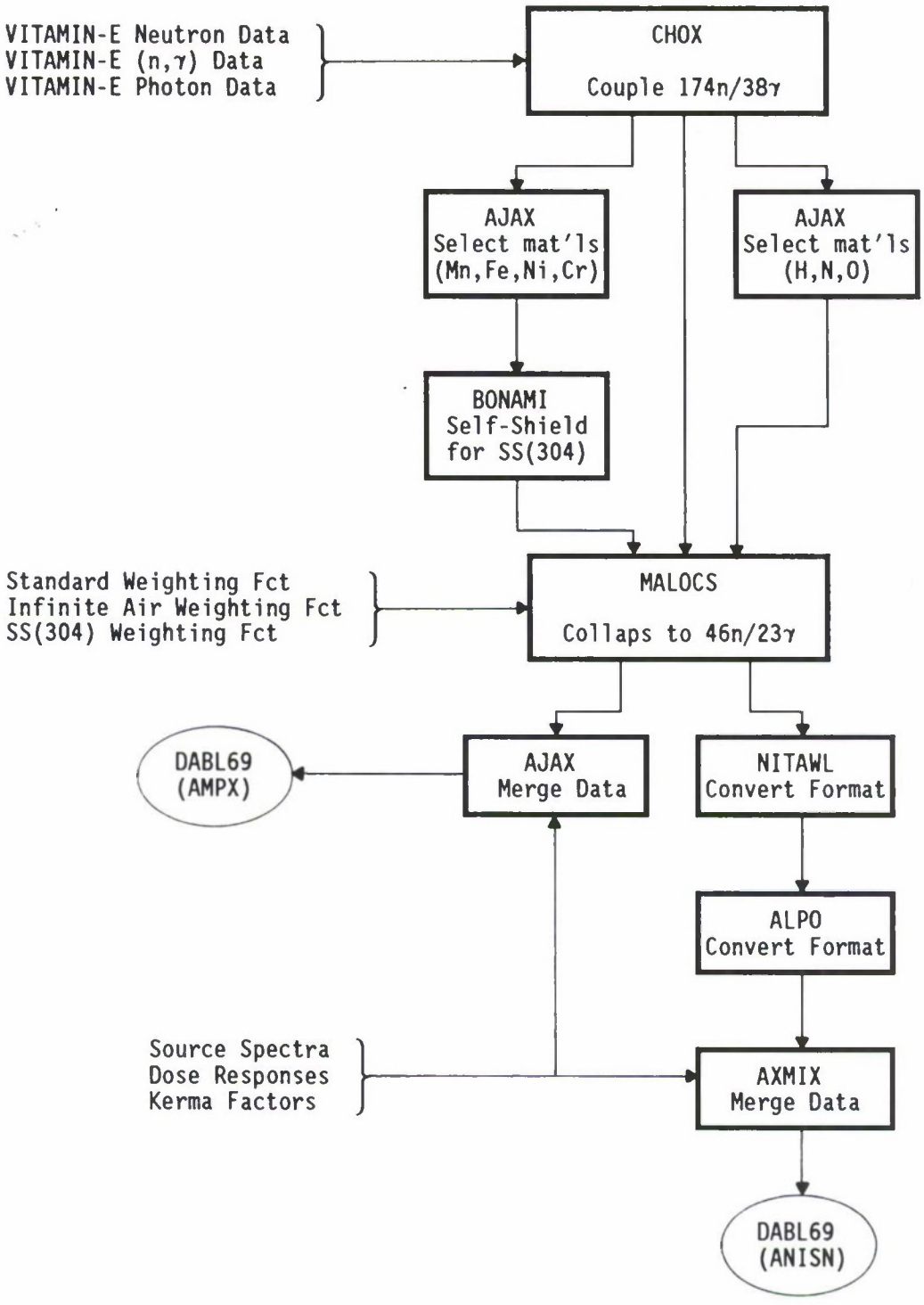

Fig. 4. Computational procedure for producing DABL69 library.

3. CONTENTS OF DABL69 LIBRARY

3.1. Contents of General Library

The full content of the DABL69 library is listed in Tables 5 and 6. Table 5 lists all of the materials which were collapsed using the standard energy weighting function. The identification numbers for both the ANISN-formatted and AMPX-formatted versions of the library are shown. Table 6 lists those special materials which were collapsed using either the infinite air weighting spectrum or the stainless steel inverse cross section weighting function. Also listed in Table 6 are the special "materials" which contain several reference source spectra and response functions. A description of these sources and responses is given in the next section.

3.2. Source Spectra and Response Data

An especially useful feature of the DLC-31 library is the inclusion of standard source spectra and response functions. This feature is continued for the new library. Source spectra include a reference fission spectrum (neutron and prompt gamma ray), a fusion spectrum, and two different unclassified weapon spectra. Responses include several different dose responses, atom displacements, and kerma factors.

In the ANISN-formatted library, the sources and responses are given in four "materials" with ID = 1000, 2000, 3000, and 4000. The contents of these materials are listed in Tables 7-10. The individual sources and responses can be retrieved according to their table positions as shown in the tables. In the AMPX-formatted library, the sources and responses are all given in Material 1000 as one dimensional arrays and are identified by a unique MT numbers which range from 9001 to 9161 (shown in parentheses in Tables 7-10). The AMPX format does not allow redundant data, i.e. data which can be derived from other existing MT data, so that responses which merely combine the separate neutron and gamma-ray components of a response (or source) into a total response are omitted from the AMPX-formatted Material 1000 (indicated as empty parentheses in the tables).

3.2.1. Reference Source Spectra

A 14-MeV source and the two unclassified weapon sources (tactical fission and thermonuclear) were originally included in the DLC-31 library.[1] The ROSIE code (unpublished) was used to interpolate and extrapolate these sources from the 37n/21γ group structure to the DABL69 46n/23γ group structure. Additionally, a ^{252}Cf source is included in the DABL69 library to provide a relatively "clean" reference fission spectrum (both neutron and prompt gamma ray). The ^{252}Cf neutron and gamma-ray spectra

TABLE 5. Materials in the DABL69 Library with Standard Weighting

Material	ID (AMPX)	ID (ANISN)	Material	ID (AMPX)	ID (ANISN)
H-1	930101	1-6	Cs-137	966901	241-246
H-2	930202	7-12	Ba-138	135301	247-252
H-3	116901	13-18	Gd	8853	253-258
He-4	127000	19-24	Hf-174	137401	259-264
Li-6	130301	25-30	Hf-176	137601	265-270
Li-7	139701	31-36	Hf-177	137701	271-276
Be-9	104	37-42	Hf-178	137801	277-282
B-10	130501	43-48	Hf-179	138301	283-288
B-11	8811	49-54	Hf-180	138401	289-294
C	130601	55-60	Ta-181	128502	295-300
N-14	127501	61-66	W-182	182	301-306
O-16	127601	67-72	W-183	183	307-312
F-19	130902	73-78	W-184	184	313-318
Na-23	131101	79-84	W-186	186	319-324
Mg	131201	85-90	Re-185	108301	325-330
Al-27	131301	91-96	Re-187	108401	331-336
Si	131401	97-102	Pt	8860	337-342
P-31	131501	103-108	Au-197	8861	343-348
S	134701	109-114	Pb	138202	349-354
Cl	114901	115-120	Bi-209	137501	355-360
Ar	8824	121-126	Th-232	139001	361-366
K	115001	127-132	Pa-233	139101	367-372
Ca	132003	133-138	U-233	139301	373-378
Ti	132201	139-144	U-234	9394	379-384
V	132301	145-150	U-235	139501	385-390
Cr	132401	151-156	U-236	139601	391-396
Mn-55	132502	157-162	U-238	139801	397-402
Fe	923604	163-168	Np-237	133701	403-408
Co-59	132703	169-174	Pu-238	133801	409-414
Ni	132802	175-180	Pu-239	139901	415-420
Cu	132901	181-186	Pu-240	138001	421-426
Ga	135801	187-192	Pu-241	138101	427-432
Y-89	920201	193-198	Pu-242	134201	433-438
Zr	8841	199-204	Am-241	136101	439-444
Nb-93	118901	205-210	Am-242	854201	445-450
Mo	132101	211-216	Am-242m	136901	451-456
Cd	8847	217-222	Am-243	136301	457-462
Sn	8850	223-228	Cm-242	864201	463-468
I-127	960601	229-234	Cm-243	134301	469-474
Cs-133	135501	235-240	Cm-244	134401	475-480

TABLE 6. Materials in the DABL69 Library with Special Energy Weighting and Special Source Spectra and Response/Kerma Functions

Material	ID (AMPX)	ID (ANISN)	Description
H-1	930121	501-506	Infinite air energy weighting[a]
N-14	127521	507-512	Infinite air energy weighting[a]
O-16	127621	513-518	Infinite air energy weighting[a]
Mo	132131	601-606	$1/[E\Sigma_T(SS)]$ energy weighting[b]
Cr	132431	607-612	$1/[E\Sigma_T(SS)]$ energy weighting[b]
Mn-55	132532	613-618	$1/[E\Sigma_T(SS)]$ energy weighting[b]
Fe	932634	619-624	$1/[E\Sigma_T(SS)]$ energy weighting[b]
Ni	132832	625-630	$1/[E\Sigma_T(SS)]$ energy weighting[b]
	1000	1000	Misc. Sources and Response Functions
	1000	2000	Elemental Kerma Factors (H - K)
	1000	3000	Elemental Kerma Factors (Ca - W)
	1000	4000	Elemental Kerma Factors (Pb - Am)

[a] Neutron flux spectrum in dry air at 2000m from a ^{252}Cf source.
[b] Standard weighting function folded with inverse of the total cross section of stainless steel (type 304).

TABLE 7. Contents of Activity Table (ID = 1000)

Table Pos.	AMPX* MT No.	Source/Response
1	(9001)	14-MeV source distribution [neutrons/source-neutron]
2	(9002)	Unclassified thermonuclear source distribution [neutrons/source-neutron]
3	(9003)	Tactical weapon fission source distribution [neutrons/source-neutron]
4	(9004)	Prompt fission gamma-ray source distribution [gammas/source-gamma]
5	( )	^{252}Cf neutron (T = 1.43 MeV) and gamma-ray (3.0625 gammas/source-neutron) source spectra
6	(9005)	^{252}Cf neutron source spectrum (T = 1.43 MeV)
7	(9006)	^{252}Cf gamma-ray source spectrum (3.0625 gammas/source-neutron)
8	( )	Kerr free-in-air tissue neutron and gamma-ray kerma factor [Gy·cm^2/n or γ]
9	(9007)	Kerr free-in-air tissue neutron kerma factor [Gy·cm^2/n]
10	(9008)	Kerr free-in-air tissue gamma-ray kerma factor [Gy·cm^2/γ]
11	( )	Active marrow neutron and gamma kerma factor [Gy·cm^2/n or γ]
12	(9009)	Active marrow neutron kerma factor [Gy·cm^2/n]
13	(9010)	Active marrow gamma-ray kerma factor [Gy·cm^2/γ]
14	( )	Small intestine neutron and gamma kerma factor [Gy·cm^2/n or γ]
15	(9011)	Small intestine neutron kerma factor [Gy·cm^2/n]
16	(9012)	Small intestine gamma-ray kerma factor [Gy·cm^2/γ]
17	( )	Si neutron and gamma-ray kerma factor [Gy·cm^2/n or γ]
18	(9013)	Si neutron kerma factor [Gy·cm^2/n]
19	(9014)	Si gamma-ray kerma factor [Gy·cm^2/γ]
20	(9015)	Si neutron ionization kerma factor [Gy·cm^2/n]
21	(9016)	Si neutron displacement kerma factor [Gy·cm^2/n]
22	(9017)	Si neutron displacement cross section [barn]
23	(9018)	Si 1-MeV-equivalent neutron displacement [dimensionless]
24	(9019)	Si gamma-ray ionization kerma factor [Gy·cm^2/γ]
25	( )	Mid-point neutron and gamma-ray group energies [eV]
26	(9020)	Mid-point neutron group energies [eV]
27	(9021)	Mid-point gamma-ray group energies [eV]
28	( )	Total neutron and gamma-ray flux
29	(9022)	Total neutron flux
30	(9023)	Total gamma-ray flux

* In AMPX format, all sources/responses are contained in one material with ID = 1000 using the indicated MT value.

TABLE 8. Contents of Activity Table (ID=2000)

Table Pos.	AMPX* MT No.	Response
1	( )	H neutron and gamma-ray kerma factor [Gy·cm^2/n or γ]
2	(9064)	H neutron kerma factor [Gy·cm^2/n]
3	(9065)	H gamma-ray kerma factor [Gy·cm^2/γ]
4	( )	He neutron and gamma-ray kerma factor [Gy·cm^2/n or γ]
5	(9066)	He neutron kerma factor [Gy·cm^2/n]
6	(9067)	He gamma-ray kerma factor [Gy·cm^2/γ]
7	( )	Li-6 neutron and gamma-ray kerma factor [Gy·cm^2/n or γ]
8	(9068)	Li-6 neutron kerma factor [Gy·cm^2/n]
9	(9069)	Li-6 gamma-ray kerma factor [Gy·cm^2/γ]
10	( )	Li-7 neutron and gamma-ray kerma factor [Gy·cm^2/n or γ]
11	(9070)	Li-7 neutron kerma factor [Gy·cm^2/n]
12	(9071)	Li-7 gamma-ray kerma factor [Gy·cm^2/γ]
13	( )	Be neutron and gamma-ray kerma factor [Gy·cm^2/n or γ]
14	(9072)	Be neutron kerma factor [Gy·cm^2/n]
15	(9073)	Be gamma-ray kerma factor [Gy·cm^2/γ]
16	( )	B-10 neutron and gamma-ray kerma factor [Gy·cm^2/n or γ]
17	(9074)	B-10 neutron kerma factor [Gy·cm^2/n]
18	(9075)	B-10 gamma-ray kerma factor [Gy·cm^2/γ]
19	( )	B-11 neutron and gamma-ray kerma factor [Gy·cm^2/n or γ]
20	(9076)	B-11 neutron kerma factor [Gy·cm^2/n]
21	(9077)	B-11 gamma-ray kerma factor [Gy·cm^2/γ]
22	( )	C neutron and gamma-ray kerma factor [Gy·cm^2/n or γ]
23	(9078)	C neutron kerma factor [Gy·cm^2/n]
24	(9079)	C gamma-ray kerma factor [Gy·cm^2/γ]
25	( )	N neutron and gamma-ray kerma factor [Gy·cm^2/n or γ]
26	(9080)	N neutron kerma factor [Gy·cm^2/n]
27	(9081)	N gamma-ray kerma factor [Gy·cm^2/γ]
28	( )	O neutron and gamma-ray kerma factor [Gy·cm^2/n or γ]
29	(9082)	O neutron kerma factor [Gy·cm^2/n]
30	(9083)	O gamma-ray kerma factor [Gy·cm^2/γ]
31	( )	F neutron and gamma-ray kerma factor [Gy·cm^2/n or γ]
32	(9084)	F neutron kerma factor [Gy·cm^2/n]
33	(9085)	F gamma-ray kerma factor [Gy·cm^2/γ]
34	( )	Na neutron and gamma-ray kerma factor [Gy·cm^2/n or γ]
35	(9086)	Na neutron kerma factor [Gy·cm^2/n]
36	(9087)	Na gamma-ray kerma factor [Gy·cm^2/γ]
37	( )	Mg neutron and gamma-ray kerma factor [Gy·cm^2/n or γ]
38	(9088)	Mg neutron kerma factor [Gy·cm^2/n]
39	(9089)	Mg gamma-ray kerma factor [Gy·cm^2/γ]

TABLE 8. Cont'd

Table Pos.	AMPX* MT No.	Response
40	( )	Al neutron and gamma-ray kerma factor [Gy·cm^2/n or γ]
41	(9090)	Al neutron kerma factor [Gy·cm^2/n]
42	(9091)	Al gamma-ray kerma factor [Gy·cm^2/γ]
43	( )	Si neutron and gamma-ray kerma factor [Gy·cm^2/n or γ]
44	(9092)	Si neutron kerma factor [Gy·cm^2/n]
45	(9093)	Si gamma-ray kerma factor [Gy·cm^2/γ]
46	( )	Cl neutron and gamma-ray kerma factor [Gy·cm^2/n or γ]
47	(9094)	Cl neutron kerma factor [Gy·cm^2/n]
48	(9095)	Cl gamma-ray kerma factor [Gy·cm^2/γ]
49	( )	K neutron and gamma-ray kerma factor [Gy·cm^2/n or γ]
50	(9096)	K neutron kerma factor [Gy·cm^2/n]
51	(9097)	K gamma-ray kerma factor [Gy·cm^2/γ]

* In AMPX format, all sources/responses are contained in one material with ID = 1000 using the indicated MT value.

TABLE 9. Contents of Activity Table (ID=3000)

Table Pos.	AMPX* MT No.	Response
1	( )	Ca neutron and gamma-ray kerma factor [Gy·cm^2/n or γ]
2	(9098)	Ca neutron kerma factor [Gy·cm^2/n]
3	(9099)	Ca gamma-ray kerma factor [Gy·cm^2/γ]
4	( )	Ti neutron and gamma-ray kerma factor [Gy·cm^2/n or γ]
5	(9100)	Ti neutron kerma factor [Gy·cm^2/n]
6	(9101)	Ti gamma-ray kerma factor [Gy·cm^2/γ]
7	( )	V neutron and gamma-ray kerma factor [Gy·cm^2/n or γ]
8	(9102)	V neutron kerma factor [Gy·cm^2/n]
9	(9103)	V gamma-ray kerma factor [Gy·cm^2/γ]
10	( )	Cr neutron and gamma-ray kerma factor [Gy·cm^2 /n or γ]
11	(9104)	Cr neutron kerma factor [Gy·cm^2/n]
12	(9105)	Cr gamma-ray kerma factor [Gy·cm^2/γ]
13	( )	Mn neutron and gamma-ray kerma factor [Gy·cm^2/n or γ]
14	(9106)	Mn neutron kerma factor [Gy·cm^2/n]
15	(9107)	Mn gamma-ray kerma factor [Gy·cm^2/γ]
16	( )	Fe neutron and gamma-ray kerma factor [Gy·cm^2/n or γ]
17	(9108)	Fe neutron kerma factor [Gy·cm^2/n]
18	(9109)	Fe gamma-ray kerma factor [Gy·cm^2/γ]
19	( )	Co neutron and gamma-ray kerma factor [Gy·cm^2/n or γ]
20	(9110)	Co neutron kerma factor [Gy·cm^2/n]
21	(9111)	Co gamma-ray kerma factor [Gy·cm^2/γ]
22	( )	Ni neutron and gamma-ray kerma factor [Gy·cm^2/n or γ]
23	(9112)	Ni neutron kerma factor [Gy·cm^2/n]
24	(9113)	Ni gamma-ray kerma factor [Gy·cm^2/γ]
25	( )	Cu neutron and gamma-ray kerma factor [Gy·cm^2/n or γ]
26	(9114)	Cu neutron kerma factor [Gy·cm^2/n]
27	(9115)	Cu gamma-ray kerma factor [Gy·cm^2/γ]
28	( )	Nb neutron and gamma-ray kerma factor [Gy·cm^2/n or γ]
29	(9116)	Nb neutron kerma factor [Gy·cm^2/n]
30	(9117)	Nb gamma-ray kerma factor [Gy·cm^2/γ]
31	( )	Mo neutron and gamma-ray kerma factor [Gy·cm^2/n or γ]
32	(9118)	Mo neutron kerma factor [Gy·cm^2/n]
33	(9119)	Mo gamma-ray kerma factor [Gy·cm^2/γ]
34	( )	Ta neutron and gamma-ray kerma factor [Gy·cm^2/n or γ]
35	(9120)	Ta neutron kerma factor [Gy·cm^2/n]
36	(9121)	Ta gamma-ray kerma factor [Gy·cm^2/γ]
37	( )	W-182 neutron and gamma-ray kerma factor [Gy·cm^2/n or γ]
38	(9122)	W-182 neutron kerma factor [Gy·cm^2/n]
39	(9123)	W-182 gamma-ray kerma factor [Gy·cm^2/γ]
40	( )	W-183 neutron and gamma-ray kerma factor [Gy·cm^2/n or γ]
41	(9124)	W-183 neutron kerma factor [Gy·cm^2/n]
42	(9125)	W-183 gamma-ray kerma factor [Gy·cm^2/γ]

TABLE 9. Cont'd

Table Pos.	AMPX* MT No.	Response
43	( )	W-184 neutron and gamma-ray kerma factor [Gy·cm^2/n or γ]
44	(9126)	W-184 neutron kerma factor [Gy·cm^2/n]
45	(9127)	W-184 gamma-ray kerma factor [Gy·cm^2/γ]
46	( )	W-186 neutron and gamma-ray kerma factor [Gy·cm^2/n or γ]
47	(9128)	W-186 neutron kerma factor [Gy·cm^2/n]
48	(9129)	W-186 gamma-ray kerma factor [Gy·cm^2/γ]

* In AMPX format, all sources/responses are contained in one material with ID = 1000 using the indicated MT value.

TABLE 10. Contents of Activity Table (ID = 4000)

Table Pos.	AMPX* MT No.	Response
1	( )	Pb neutron and gamma-ray kerma factor [Gy·cm^2/n or γ]
2	(9130)	Pb neutron kerma factor [Gy·cm^2/n]
3	(9131)	Pb gamma-ray kerma factor [Gy·cm^2/γ]
4	( )	Th-232 neutron and gamma-ray kerma factor [Gy·cm^2/n or γ]
5	(9132)	Th-232 neutron kerma factor [Gy·cm^2/n]
6	(9133)	Th-232 gamma-ray kerma factor [Gy·cm^2/γ]
7	( )	Pa neutron and gamma-ray kerma factor [Gy·cm^2/n or γ]
8	(9134)	Pa neutron kerma factor [Gy·cm^2/n]
9	(9135)**	Pa gamma-ray kerma factor [Gy·cm^2/γ]
10	( )	U-233 neutron and gamma-ray kerma factor [Gy·cm^2/n or γ]
11	(9136)	U-233 neutron kerma factor [Gy·cm^2/n]
12	(9137)	U-233 gamma-ray kerma factor [Gy·cm^2/γ]
13	( )	U-234 neutron and gamma-ray kerma factor [Gy·cm^2/n or γ]
14	(9138)	U-234 neutron kerma factor [Gy·cm^2/n]
15	(9139)	U-234 gamma-ray kerma factor [Gy·cm^2/γ]
16	( )	U-235 neutron and gamma-ray kerma factor [Gy·cm^2/n or γ]
17	(9140)	U-235 neutron kerma factor [Gy·cm^2/n]
18	(9141)	U-235 gamma-ray kerma factor [Gy·cm^2/γ]
19	( )	U-236 neutron and gamma-ray kerma factor [Gy·cm^2/n or γ]
20	(9142)	U-236 neutron kerma factor [Gy·cm^2/n]
21	(9143)	U-236 gamma-ray kerma factor [Gy·cm^2/γ]
22	( )	U-238 neutron and gamma-ray kerma factor [Gy·cm^2/n or γ]
23	(9144)	U-238 neutron kerma factor [Gy·cm^2/n]
24	(9145)	U-238 gamma-ray kerma factor [Gy·cm^2/γ]
25	( )	Np neutron and gamma-ray kerma factor [Gy·cm^2/n or γ]
26	(9146)	Np neutron kerma factor [Gy·cm^2/n]
27	(9147)**	Np gamma-ray kerma factor [Gy·cm^2/γ]
28	( )	Pu-238 neutron and gamma-ray kerma factor [Gy·cm^2 /n or γ]
29	(9148)	Pu-238 neutron kerma factor [Gy·cm^2/n]
30	(9149)	Pu-238 gamma-ray kerma factor [Gy·cm^2/γ]
31	( )	Pu-239 neutron and gamma-ray kerma factor [Gy·cm^2/n or γ]
32	(9150)	Pu-239 neutron kerma factor [Gy·cm^2/n]
33	(9151)	Pu-239 gamma-ray kerma factor [Gy·cm^2/γ]
34	( )	Pu-240 neutron and gamma-ray kerma factor [Gy·cm^2/n or γ]
35	(9152)	Pu-240 neutron kerma factor [Gy·cm^2/n]
36	(9153)	Pu-240 gamma-ray kerma factor [Gy·cm^2/γ]
37	( )	Pu-241 neutron and gamma-ray kerma factor [Gy·cm^2/n or γ]
38	(9154)	Pu-241 neutron kerma factor [Gy·cm^2/n]
39	(9155)	Pu-241 gamma-ray kerma factor [Gy·cm^2/γ]
40	( )	Pu-242 neutron and gamma-ray kerma factor [Gy·cm^2/n or γ]
41	(9156)	Pu-242 neutron kerma factor [Gy·cm^2/n]
42	(9157)	Pu-242 gamma-ray kerma factor [Gy·cm^2/γ]

TABLE 10. Cont'd

Table Pos.	AMPX* MT No.	Response
43	( )	Am-241 neutron and gamma-ray kerma factor [Gy·cm^2/n or γ]
44	(9158)	Am-241 neutron kerma factor [Gy·cm^2/n]
45	(9159)**	Am-241 gamma-ray kerma factor [Gy·cm^2/γ]
46	( )	Am-243 neutron and gamma-ray kerma factor [Gy·cm^2/n or γ]
47	(9160)	Am-243 neutron kerma factor [Gy·cm^2/n]
48	(9161)**	Am-243 gamma-ray kerma factor [Gy·cm^2/γ]

* In AMPX format, all sources/responses are contained in one material with ID = 1000 using the indicated MT value.
** No data at present

are based on measurements made in air at approximately 2m from a small "needle" source of californium.[10,11] The neutron spectrum was first generated in the VITAMIN-E group structure by group-wise integration of the Maxwellian distribution which had been fitted to the measured neutron spectrum.[10] Similarly, the gamma-ray spectrum was generated by group-wise integration of the exponential function which had been empirically fitted to the measured gamma-ray spectrum.[11] The measured source strength from the Cf needle yielded a normalization of 3.0625 gamma rays per source neutron. Both the neutron and gamma-ray spectra were then converted from the VITAMIN-E group structure into the DABL69 structure using ROSIE.

The four neutron source spectra are shown in Fig. 5 and the two gamma-ray source spectra are shown in Fig. 6. The gamma-ray spectra are surprisingly similar despite their different origins.

3.2.2. Reference Response Functions

The DLC-31 library contains a number of useful response functions. Some of the outdated responses have been dropped for DABL69, while other new responses have been added. Although many of the responses are based largely on ENDF/B-IV or earlier data, it is still useful to distribute them with the new library. As new response functions are computed with improved data, they will be incorporated into the library.

An explanation for the origin of the various responses and pertinent qualifications for the data are as follows:

Kerr free-in-air tissue kerma factors: These were collapsed from 174n/38γ data[12] using the RIPOF program.[13] The weighting functions used for the collapsing were the VITAMIN-E weighting function for neutron groups and a 1/E weighting function for gamma-ray groups. The 174n/38γ data had been interpolated/extrapolated from the original 112n/35γ data of Kerr[14] using the ROSIE code. The units for these factors are $Gy \cdot cm^2/n$ for neutrons and $Gy \cdot cm^2/\gamma$ for gamma rays. These are the units to be adopted for all other kerma factors described below.

Active marrow and small intestine kerma factors: These are for a 57-kg phantom isotropically exposed to monoenergetic radiative particles. The original data,[15] which were in the VITAMIN-E energy group structure, contained zeros in the first two neutron groups and the first gamma-ray group. This was a consequence of special considerations relevant to the application for which the responses were generated and is not appropriate for general use. Therefore, the zero values were replaced by values obtained using the assumption that the respective shielded and free-in-air kerma factors are proportional for the first three groups. The resulting 174n/38γ data were then collapsed using

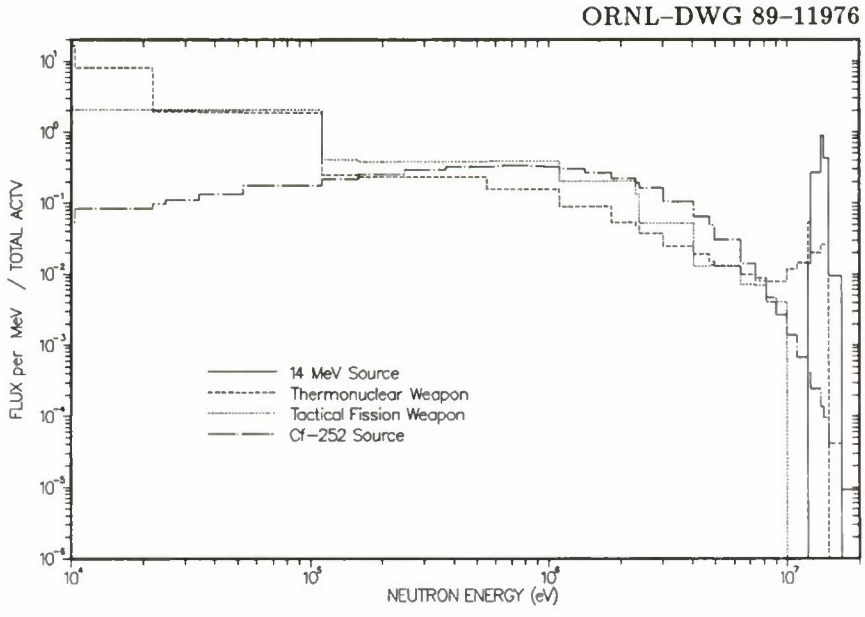

Fig. 5. Neutron source spectra included in material with ID = 1000.

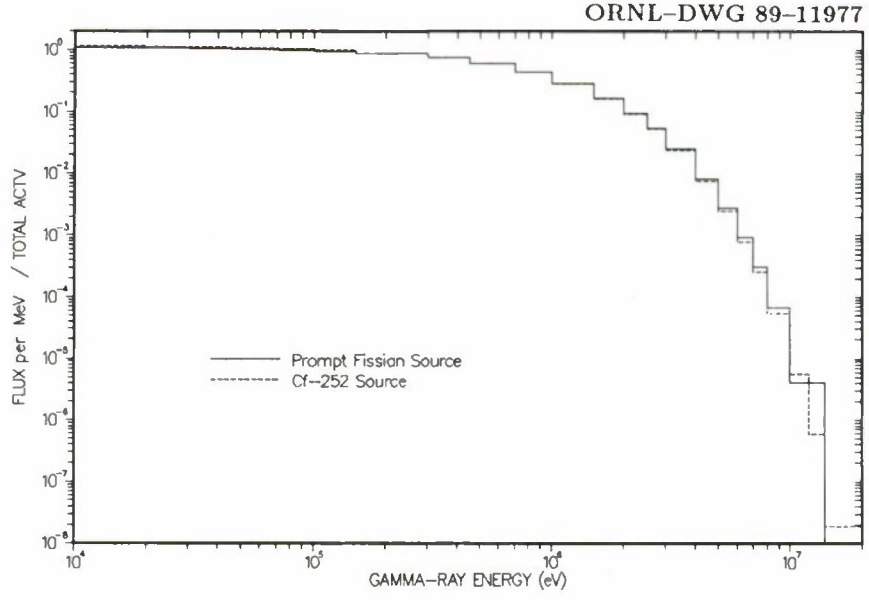

Fig. 6. Gamma-ray source spectra included in material with ID = 1000.

RIPOF. The weighting functions used for collapsing were the VITAMIN-E weighting function for neutron groups and a 1/E weighting function for gamma-ray groups.

Silicon neutron kerma factors: These were evaluated from three sources, all based on ENDF/B-IV. These include the 112-group data of Caswell et al.,[16] the point data of Verbinski et al.,[17] and the 171-group data in MACKLIB-IV.[13] The data of Caswell et al. and MACKLIB-IV were both expanded into the VITAMIN-E group structures using ROSIE and then collapsed into the present structure using RIPOF and the VITAMIN-E weighting function. The data of Caswell et al. have been multiplied by 0.01 to convert from Rad/(n/cm^2) to Gy·cm^2/n. The data of MACKLIB-IV have been multiplied by 3.446 x 10^{-18} to change from eV·b/atom to Gy·cm^2/n. The point data of Verbinski et al. were first converted into the ENDF/B-V format assuming log-log interpolation,[12] then processed into the VITAMIN-E group structure using the AMPX module VEL,[18] and finally collapsed into the present group structure using RIPOF. These data have been multiplied by 3.446 x 10^{-15} to change from MeV·mb/atom to Gy·cm^2/n. The three sets of data in 46-group structure were compared and found to be in reasonable group-wise agreement (20-40%) except the last seven groups, for which the data in MACKLIB-IV are larger than the others by factors of 2 to 20. This larger result was suspected to be due to the fact that the calculation of the (n,γ) kerma factor in MACKLIB-IV was based on the recoil of a single gamma-ray rather than a realistic distributed gamma-ray emission as considered by the others, thus yielding much larger recoil. Therefore, the recommended values were obtained by averaging the three sets for groups 1 to 39 and by averaging only the data of Caswell et al. and Verbinski et al. for groups 40 to 46.

Silicon gamma-ray kerma factors: These were taken from the 36-gamma-ray group MACKLIB-IV data for Si. See explanation below for "Elemental kerma factors."

Silicon neutron ionization kerma factors: These were taken to be the differences between the evaluated total neutron kerma factors and the evaluated neutron displacement kerma factors for Si, described below.

Silicon neutron displacement kerma factors: These are averages of the Verbinski et al. data[17] and data by Gabriel.[19] The point data of Verbinski et al. were processed in the same manner as described above for the total kerma factors. The Gabriel displacement cross sections in barns were divided by 0.016 to get displacement kerma factors in eV·b/atom, which were then multiplied by 3.446 x 10^{-18} to convert to Gy·cm^2/n. The Gabriel data are in the 105-group structure and were processed into 46 groups using ROSIE and RIPOF as above.

Silicon neutron displacement cross sections: These were converted from the displacement kerma factors in $Gy \cdot cm^2/n$ which were divided by 3.446×10^{-18} to get $eV \cdot b/atom$ and multiplied by 0.016 to convert to displacement cross sections in barns.

Silicon 1-MeV-equivalent neutron displacement: These are ratios of Si neutron displacement cross sections to the 1-MeV value, which was taken to be that for the 22nd group (0.962 to 1.11 MeV), i.e., 1316 barns.

Silicon gamma-ray ionization kerma factors: These were converted from the DLC-31 21-group gamma-ray data using ROSIE. The data have been multiplied by 0.01 to change from $Rad/(\gamma/cm^2)$ to $Gy \cdot cm^2/\gamma$.

Elemental kerma factors: The 171n/36γ MACKLIB-IV library was expanded to the 174n/38γ structure using ROSIE. The resulting data were then collapsed to the 46n/23γ structure using RIPOF. The weighting functions used for the collapsing were the VITAMIN-E weighting for neutron and the 1/E weighting function for gamma-ray. The data have been multiplied by $9.649 \times 10^{-17}/A$ to change from $eV \cdot b/atom$ to $Gy \cdot cm^2/n$ for neutron or $Gy \cdot cm^2/\gamma$ for gamma ray (A = atomic mass of the particular element). All elemental kermas ranging from H-1 to Am-243 were obtained this way, excepting for Si neutron kerma factors, which have been evaluated more carefully as discussed above. The data entered in ID = 2000 for Si are identical to those in ID = 1000.

4. TESTING OF DABL69 CROSS SECTIONS

Of utmost importance in the generation of the DABL69 library was the reliability of the final cross sections. As stated in previous sections, using the thoroughly tested VITAMIN-E fine-group data as the starting point for DABL69 and using proven modules of the AMPX code system to collapse and process the data contributes substantially to the reliability of the library. In addition, specific calculations were performed with the new cross sections and compared to results from similar calculations performed using other cross sections such as the older DLC-31 data. These kinds of comparisons provide "qualitative" testing of the library since the two solutions are not expected to agree, hopefully due to the better data represented in the new cross sections. Such comparisons do help to identify errors in the processing, which usually manifest themselves in solutions which are clearly erroneous. Ultimately, testing of the new data against integral experiments is needed to demonstrate quantitative accuracy. It is expected that all of these forms of testing will be accomplished for DABL69, facilitated by its wide distribution and use throughout the DNA radiation transport community.

As an initial test of the library, several air transport calculations were performed. Transport of neutrons and gamma rays through 3000m of dry air was calculated using the ANISN code. The reference Cf-252 neutron and prompt gamma-ray sources contained within the library were used as the source spectra. Actually, four different calculations were performed for each of the neutron and gamma-ray sources. These cases used different group structures, weighting functions or data. For the neutron transport, the four cases included: (1) the VITAMIN-E 174-group cross sections, (2) the DABL69 46-group cross sections weighted by the standard weighting function, (3) the DABL69 46-group cross sections weighted by the infinite air weighting function, and (4) the DLC-31 37-group cross sections weighted by a weapon fission spectrum. For the gamma-ray transport, the four cases included: (1) the VITAMIN-E 38-group cross sections, (2) the DABL69 23-group cross sections weighted by the 1/E weighting function, (3) the DABL69 23-group cross sections weighted by a flat weighting function (not used in the library), and (4) the DLC-31 21-group cross sections weighted by a flat weighting function.

Figure 7 compares results from the four neutron transport problems. In each case, the neutron flux at each spatial point has been folded with the Kerr soft tissue kerma response and then computed as a percent difference from the reference VITAMIN-E results. The older DLC-31 cross sections appear to yield an excellent agreement with the fine-group results at 3000m, but show nearly an 8% overprediction of the response at interim ranges. On the other hand, the standard-weighted DABL69 cross sections give a uniformly increasing underprediction of the fine-group results with a maximum difference of 12% occurring at 3000m. The best agreement was

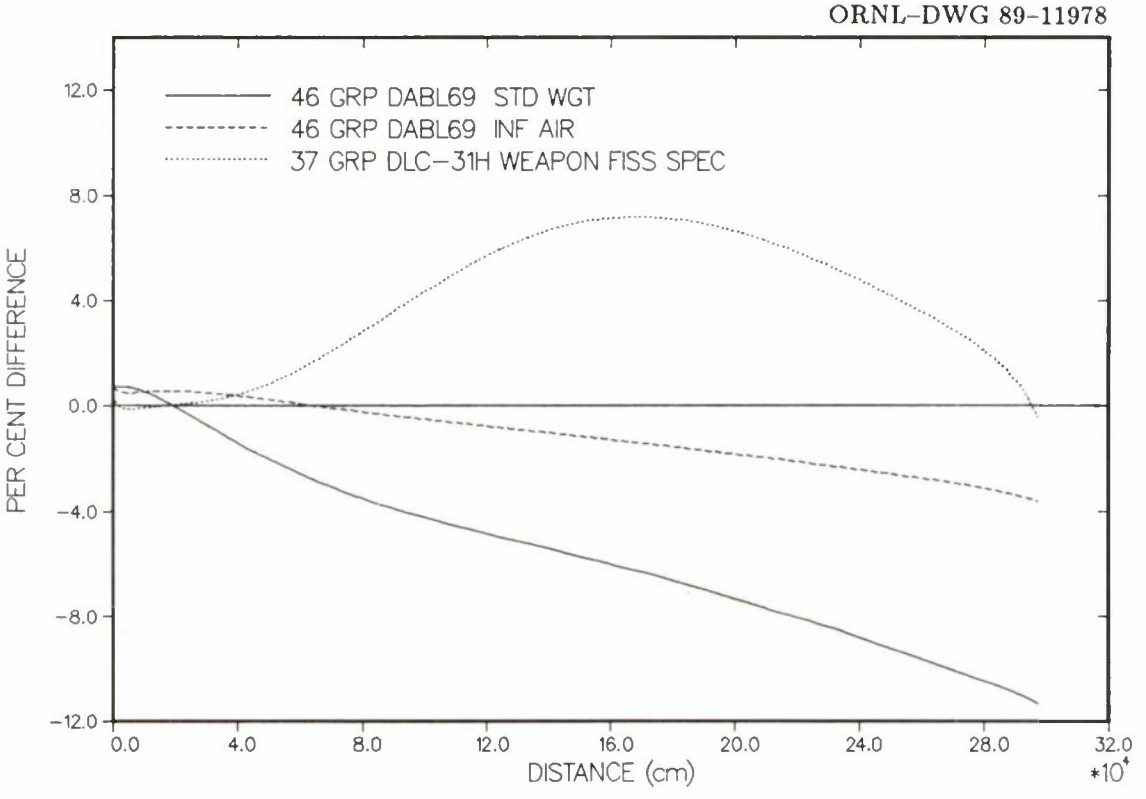

Fig. 7. Soft tissue neutron kerma response calculated in dry air from a Cf-252 fission neutron source compared to reference VITAMIN-E results.

achieved with the air-weighted DABL69 cross sections, which gave only a 4% difference from the VITAMIN-E data.

Similar comparisons are given in Fig. 8 for the gamma-ray transport problem. Both the flat-weighted DLC-31 and DABL69 data yielded substantially poorer agreement with the fine-group data than did the 1/E-weighted DABL69 data. As with the neutron problems, an agreement of better than 5% was achieved, even using only a single energy weighting of the few-group data for the full 3000m range.

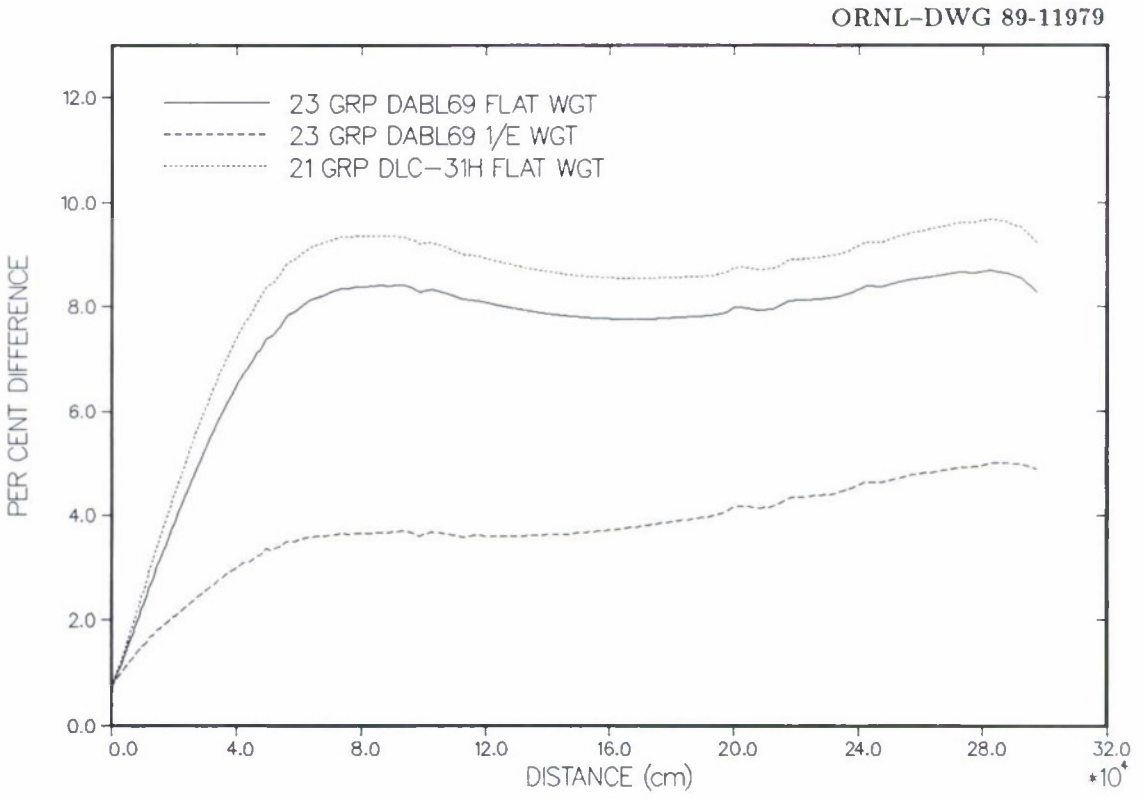

Fig. 8. Soft tissue gamma-ray kerma response calculated in dry air from a Cf-252 fission prompt gamma-ray source compared to reference VITAMIN-E results.

REFERENCES

1. D. E. Bartine, J. R. Knight, J. V. Pace, III, and R. W. Roussin, *Production and Testing of the DNA Few-Group Coupled Neutron-Gamma Cross-Section Library*, ORNL/TM-4840 (1977). Available from RSIC as DLC-31/(DPL-1/FEWG1).

2. Private correspondence from D. Kaul, SAIC to Major J. Campbell, DNA, March 30, 1984.

3. Private correspondence from D. Kaul, SAIC to J. Marcum, RDA, September 18, 1984.

4. C. R. Weisbin, et al, *VITAMIN-E: An ENDF/B-V Multigroup Cross-Section Library for LMFBR Core and Shield, LWR Shield, Dosimetry, and Fusion Blanket Technology*, ORNL-5505 (February 1979).

5. N. M. Greene, et al, *AMPX: A Modular Code System for Generating Coupled Multigroup Neutron-Gamma Libraries from ENDF/B*, ORNL/TM-3706 (1976).

6. C. Y. Fu and D. M. Hetrick, *Update of ENDF/B-V Mod-3 Iron: Neutron-Producing Reaction Cross Sections and Energy-Angle Correlations*, ORNL/TM-9964 (July 1986).

7. W. W. Engle, Jr., *A User's Manual for ANISN - A One-Dimensional Discrete Ordinates Transport Code with Anisotropic Scattering*, Oak Ridge Gaseous Diffusion Plant Report, K-1693 (1967).

8. M. B. Emmett, *The MORSE Monte Carlo Radiation Transport Code System*, ORNL-4972 (February 1975).

9. S. N. Cramer, "Adjoint Gamma-Ray Estimation to the Surface of a Cylinder - Analysis of a Remote Reprocessing Facility," *Nucl. Sci. and Eng.* **79**, 417-425 (1981).

10. R. H. Johnson, D. T. Ingersoll, B. W. Wehring, and J. J. Dorning, "NE-213 Neutron Spectrometry System For Measurements From 1.0 to 20 MeV," *Nucl. Instr. and Meth.* **145**, 337-346 (1977).

11. D. T. Ingersoll and B. W. Wehring, "Gamma-Ray Pulse-Height Response of an NE-213 Scintillation Detector," *Nucl. Instr. and Meth.* **147**, 551-561 (1977).

12. J. V. Pace, Private Communication (1986).

13. Y. Gohar and M. A. Abdou, *MACKLIB-IV, A Library of Nuclear Response Functions Generated with the MACK-IV Computer Program from ENDF/B-IV*, ANL/FPP/TM-106 (1978).

14. G. D. Kerr, *Photon and Neutron Fluence-To-Kerma Conversion Factors for ICRP-1975 Reference Man Using Improved Elemental Compositions for Bone and Marrow of the Skeleton*, ORNL/TM-8318 (1982).

15. J. C. Ryman, M. Cristy, K. F. Ekerman, J. L. Davis, J. S. Tang, and G. D. Kerr, "A Code System to Compute Radiation Dose in Human Phantoms," *Trans. Am. Nuc. Soc.* **53**, 37 (1986), and Private Communication (1986).

16. R. S. Caswell, J. J. Coyne, and M. L. Randolph, "Kerma Factors for Neutron Energies below 30 MeV," *Rad. Res.* **83**, 217 (1980).

17. V. V. Verbinski, N. A. Lurie, and V. C. Rogers, "Threshold-Foil Measurement of Reactor Neutron Spectra for Radiation Damage Applications," *Nucl. Sci. Eng.* **65**, 316 (1978).

18. N. M. Greene, unpublished module VEL of the AMPX code system (ORNL/TM-3706, 1976), Private Communication (1986).

19. T. A. Gabriel, J. D. Amburgey, and N. M. Greene, *Radiation-Damage Calculations: Primary Recoil Spectra, Displacement Rates, and Gas-Production Rates*, ORNL/TM-5160 (1976).

ORNL/TM-10568

INTERNAL DISTRIBUTION

1. R. G. Alsmiller
2. B. R. Appleton
3. Y. Y. Azmy
4. D. E. Bartine
5. R. L. Childs
6. S. N. Cramer
7. M. B. Emmett
8. W. W. Engle, Jr.

9-13. C. Y. Fu

10-14. D. T. Ingersoll

15. J. O. Johnson
16. G. D. Kerr
17. R. A. Lillie
18. F. C. Maienschein
19. J. V. Pace III
20. C. V. Parks
21. S. A. Raby
22. W. A. Rhoades

23-27. R. W. Roussin

28. J. C. Ryman
29. R. T. Santoro
30. C. O. Slater
31. R. M. Westfall

32-36. J. E. White

37. L. R. Williams

38-40. Laboratory Records Department

41. Laboratory Records, ORNL-RC
42. Document Reference Section
43. Central Research Library
44. ORNL Patent Section

45. Office of the Assistant Manager for Energy Research and Development, DOE-ORO, Oak Ridge TN 37831.

46. D. Auton, Defense Nuclear Agency, ATTN: STRP, 6801 Telegraph Road, Alexandria VA 22310.

47. J. J. Dorning, Department of Nuclear Engineering and Engineering Physics, Thornton Hall, University of Virginia, Charlottesville, Virginia 22901.

48. R. M. Haralick, Department of Electrical Engineering, University of Washington, Seattle, Washington 98195.

49. D. C. Kaul, Science Applications , Manager, Radiation Physics Division, 10260 Campus Point Drive, San Diego CA 92121.

50. S. Levin, P.O. Box 547, Espanola NM 87532.

51. R. L. Stohler, Dikewood Division, Kaman Sciences Corporation, 6400 Upton Blvd., NE, Suite 300E, Albuquerque NM 87110.

52. R. W. Young, Defense Nuclear Agency, ATTN: STRP, 6801 Telegraph Road, Alexandria VA 22310.

53-379. Defense Nuclear Agency Transport Distribution (AU).

380-389. Office of Scientific and Technical Information, P.O. Box 62, Oak Ridge TN 37830.